Biophysical Chemistry 10 (1979) 289–303
© North-Holland Publishing Company

THE BINDING OF A NEUTRAL AROMATIC MOLECULE TO A NEGATIVELY-CHARGED LIPID MEMBRANE.
I. THERMODYNAMICS AND MODE OF BINDING

Paul WOOLLEY*
Magdalene College, Cambridge, England,
and Max-Planck-Institut für biophysikalische Chemie, Göttingen, West Germany

Received 4 December 1978
Revised manuscript received 6 March 1979

This paper presents a detailed study of the binding of the fluorescent dye N-phenyl naphthylamine (NPN) to bilayers composed of the negatively-charged phospholipid methylphosphatidic acid. Binding to the liquid-crystalline membrane is enthalpy-driven. It is shown by determination of the binding constant and confirmed by n.m.r. that most of the dye ("guest") molecules reside between the lipid hydrocarbon chains at a fixed distance from the head-group, and are not distributed uniformly throughout the hydrocarbon phase. Each guest molecule is surrounded by about four lipid molecules. Transition of the membrane from the liquid-crystalline to the crystalline state results in almost total expulsion of the bound NPN into the water phase. Electrostatic theory is developed to find the effect of electrostatics upon the binding of a neutral molecule to charged membranes. Although the charge product is zero, electrostatic interactions play a part in determining the strength of binding, if each guest molecule incorporated increases the area of the membrane. For NPN this increase was found to be ca. 41 Å^2.

1. Introduction

This study was prompted by the increasing use of fluorescent dyes to monitor the physical state of lipid bilayers in dispersed form, and in particular by the use of N-phenyl naphthylamine (NPN, fig. 1) in various laboratories. The indicator NPN expresses in its fluorescence quantum yield the polarity of its environment, and the intensity of the light output from the dye in the presence of most phospholipids shows a sharp rise accompanying the crystal-liquid crystal ("ordered-fluid") phase transition. This rise is presumed [1] to correspond to entry of the dye from the aqueous phase into the non-polar interior of the membrane.

In view of the increasing use of this dye, both as a static indicator of the state of the lipid bilayer and as a dynamic indicator of the progress of the phase transition [2], it was felt necessary to find out as far as possible (i) the thermodynamic forces determining the binding of the indicator to the membrane and the

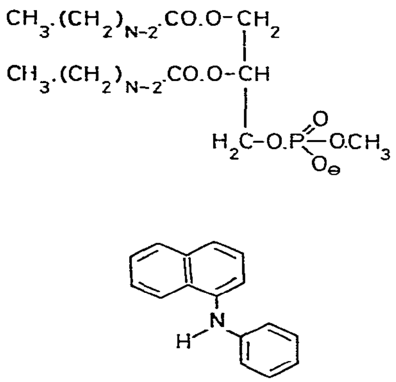

Fig. 1. Structures of C_N-MPA and NPN. in NPN there is restricted rotation about the C–N bonds; owing to steric interference the phenyl and naphthyl rings are not quite coplanar.

---

* Present address: Max-Planck-Institut für molekulare Genetik, Berlin 33.

detailed changes that enable it to differentiate between crystalline and liquid-crystalline states of the bilayer, (ii) the placing and configuration of the dye when it is bound in or on the membrane and (iii) the rate at which the dye associates with and dissociates from the membrane. This paper deals with points (i) and (ii), while the kinetics are described in the following paper.

These matters were investigated using the lipid methyl-phosphatidic acid (MPA), the methyl ester of phosphatidic acid (fig. 1). This lipid has already been extensively employed to study electrostatic phenomena at the surface of lipid membranes and their influence upon the phase transition [3,4], proton [3,4] and calcium ion [5] binding, phase separation [6] and possible enzyme regulation [7]. Consequently a detailed knowledge of the MPA—NPN interaction was of particular interest.

2. Materials and methods

2.1. Preparation of MPA

Lecithins (Fluka) were converted into MPA by digestion with white cabbage phospholipase D in the presence of methanol, according to the procedure of Kovatchev [8]. The MPA was purified by extraction with a chloroform, methanol and water mixture (by volume 1 : 1.2 : 1) and chromatography over a silica column (Merck Kieselgel 60). The column was packed and loaded using a 1 : 1 mixture of hexane and diisopropyl ether and elution was carried out in a mixture of 200 : 15 : 1 : 0.1 parts of chloroform, methanol, water and concentrated aqueous ammonia; during elution the proportion of chloroform was reduced gradually to 65 parts. The product was kept around pH 8 at all times. Fractions were identified using thin-layer chromatography. The pure MPA fraction was evaporated to dryness and redissolved in the smallest possible amount of chloroform, to which a tenfold volume of acetone was added. Crystals of MPA appeared on standing at 5°C. Dilauroyl, dimyristoyl, dipalmitoyl and distearoyl MPA's were prepared in this manner; the efficiency of the recrystallisation increased markedly with increasing chain length. The yield, starting from 1 g lecithin, was typically 500 mg (55%).

2.2. Purity

MPA, synthesized as above, was checked for purity by thin layer chromatography. No appreciable contamination was present. Further, the temperatures of the phase transition were checked for the various MPA's (this is another criterion of freedom from trace organic contaminants). These were satisfactory; values at neutral pH were: C_{12}-MPA, 5°C; C_{14}-MPA, 28°C; C_{16}-MPA, 49°C; C_{18}-MPA, 61°C. There may have been slight contamination of the C_{18}-MPA, since the value is a little low and the hysteresis was greater than in the other three cases.

Sodium chloride was from Merck ("Suprapur" grade). NPN, supplied by Kodak, was used without further purification in the titration and kinetic experiments, and recrystallized once from aqueous ethanol for the determination of its solubility. Water was used direct from a quartz double still.

2.3. Preparation of dispersions

In order to be sure of reproducible results, a standard procedure, due to U. Strehlow, was adopted for the preparation of the dispersions. A weighed amount of pure lipid and the required amount of water were placed in a 5 ml polystyrene tube, which was then sealed. The tube was shaken gently in order to wet the lipid thoroughly and then incubated at 70°C for one hour, with further shaking every 20—30 minutes. After this the tube was clamped so as to immerse it as deeply as possible into the bath attachment of a Branson Sonifier B-12. Sonication at minimum power was then carried out for ten minutes; the temperature of sonication was 30°C for C_{12}- and C_{14}-MPA's, 55°C for C_{16}-MPA and 70°C for C_{18}-MPA. (High temperatures were generally avoided in order to minimize any possible chemical decomposition, but higher temperatures were needed for the latter lipids in order to disperse them in the fluid state.) After sonication the tube was incubated at 70°C for a further 1—2 hours in order to anneal the bilayers. If a larger volume of dispersion was required then the dispersion was diluted down after sonication and the annealing carried out on the diluted dispersion, to ensure full equilibration. Only after annealing was salt added; the kinetic properties of the salt-free dispersions (see accompanying paper) were unaltered after one week of storage at 5°C, whereas noticable flocculation took place within 48 hours in the presence of 0.1 M sodium chloride.

The product of "standard sonication" is a dispersion containing principally small bilayer vesicles (see accompanying paper, fig. 6).

For some dispersions of C_{14}-MPA, with which the binding constant to NPN below the transition temperature was to be measured, a much milder sonication procedure was used: the lipid-water mixture after the first incubation was sonicated in a glass container by immersion in an ultrasound cleaning bath (the glass absorbs a substantial fraction of the sound energy). The reason for this is discussed below (sect. 4.1).

The effect of sucrose on the transition temperature of C_{14}-MPA was investigated in order to ensure that the use of sucrose to increase viscosity does not destroy the bilayer. A dispersion of MPA containing (as in the kinetic measurements) 0.1 M NaCl and 10^{-3} M Na_2HPO_4 showed transition temperatures of 27°C in water, 28.5°C in 25% w/w sucrose–water and 32°C in 50% w/w sucrose–water. The forms of all three curves were the same, and the slight raising of the transition temperature may be attributed to phosphate–sugar–phosphate hydrogen bonding [9]. This was taken as evidence that surcrose does not damage the bilayer. The binding constants in the presence of sucrose are used in the evaluation of kinetic data (see accompanying paper).

2.4. Sample handling

NPN, owing to its sparing solubility in water, was dissolved in methanol and the methanolic solution was added with a glass (Pederson) micropipette to the aqueous dispersion or solution. When this is done, a cloudy, colloidal precipitate of NPN forms, which redissolves within a few seconds. Although the solubility of NPN in equilibrium with the crystal is only around 10^{-5} M, it is possible by the above method to obtain supersaturated solutions which are stable enough for the experiments in question and which contain up to 3×10^{-5} M NPN. Above this concentration the colloidal precipitate does not redissolve. The stability of the supersaturated solutions is not due to the small quantity of methanol present ($\leqslant 1\%$), since the NPN remained in solution during the titration at 70°C, at which temperature the methanol evaporates off.

MPA and NPN were always added to a reaction mixture as late as possible, in order to avoid possible flocculation, photolysis, etc. NPN solutions were kept in the dark; these, MPA dispersions and all solutions containing sucrose were stored at 5°C.

2.5. Determination of NPN solubility

Commercial NPN was recrystallised from aqueous ethanol and large, needleshaped crystals were obtained. A few of these were incubated for a week (with occasional shaking) at 20°C in the dark, in 10 ml of sodium chloride solutions of the desired concentrations. The solutions were then pipetted into UV-quartz cells, leaving the crystals behind, and their UV spectra were taken with an Pye Unicam SP 1800 spectrophotometer at ca. 30°C (above 20°C to prevent crystallisation). The extinction coefficients were also checked at these salt concentrations using standard NPN solutions.

2.6. Titration to determine NPN/MPA binding constants

Fluorimetric titrations were carried out with a Fica 55 spectrofluorimeter. The wavelengths of excitation and emission were respectively 330 and 415 nm. The entrance slit was stopped down to a bandwidth of 2.5 nm in order to minimise photolysis of the NPN, and the excitation beam was cut off except when a reading was being taken. Photolysis during titration was thus reduced to a negligible level. A good signal/noise ratio was obtained with an exit slit of 7.5 nm bandwidth.

In a typical experiment, the solution to be titrated contained 1 mM disodium hydrogen phosphate as buffer, the required amount of sodium chloride, 5×10^{-6} M NPN and enough water to bring the volume to 2 ml. This was placed in a stoppered cell ("Suprasil" grade quartz, 1 cm × 1 cm) and its fluorescence signal was monitored. This is the signal due to NPN in water alone. Small volumes of MPA dispersions (10^{-3} or 10^{-2} M) were then added using an Eppendorf micropipette and the measurement repeated. The pH was ca 7.6, corresponding to fully ionised MPA at this salt concentration. Each signal was plotted against time on a chart recorder and a time-average (estimated by eye) over 100 seconds was taken. Checks were made to ensure adequate thermal equilibration.

3. Results

3.1. Equilibrium binding of NPN to fluid MPA

The binding constants are defined by eq. (1), which holds when MPA is in excess over bound NPN. [MPA] is expressed as the total number of moles of lipid per litre (other ways of expressing this, which take account of the nature of the binding, are discussed below). No distinction is made between "bound" and "free" MPA, since it is in excess,

$$K = \frac{[\mathrm{NPN_{bound}}]}{[\mathrm{NPN_{free}}]} \cdot \frac{1}{[\mathrm{MPA}]} \,. \qquad (1)$$

Of the standard and the gentle sonication procedures (sect. 2.3), the former produces smaller vesicles. These cause less light-scattering than do the larger ones, making them better suited for fluorescence measurements.

A representative family of titration curves is shown in fig. 2. C_{12}- and other MPA's studied in the fluid state gave sufficiently accurate titration curves to allow evaluation of the parameters of binding by computer-aided least-squares refinement. The programme adjusted $\Delta F_{\max}$ and K in eq. (2) to fit the observed fluorescence intensity F (see table 1). F is not corrected for internal absorption, since this was small ($\leqslant$ 0.1 O.D. units) and constant. F_0 is the observed fluorescence in water of NPN alone. The final factor in eq. (2) is a dilution correction, where v is the volume of MPA solution added to the 2 ml sample at any stage in the titration. The correction is exact when the dye is almost completely bound ([MPA] $\approx 10^{-3}$ M) and, under the conditions of the experiment, negligible at other concentrations of MPA.

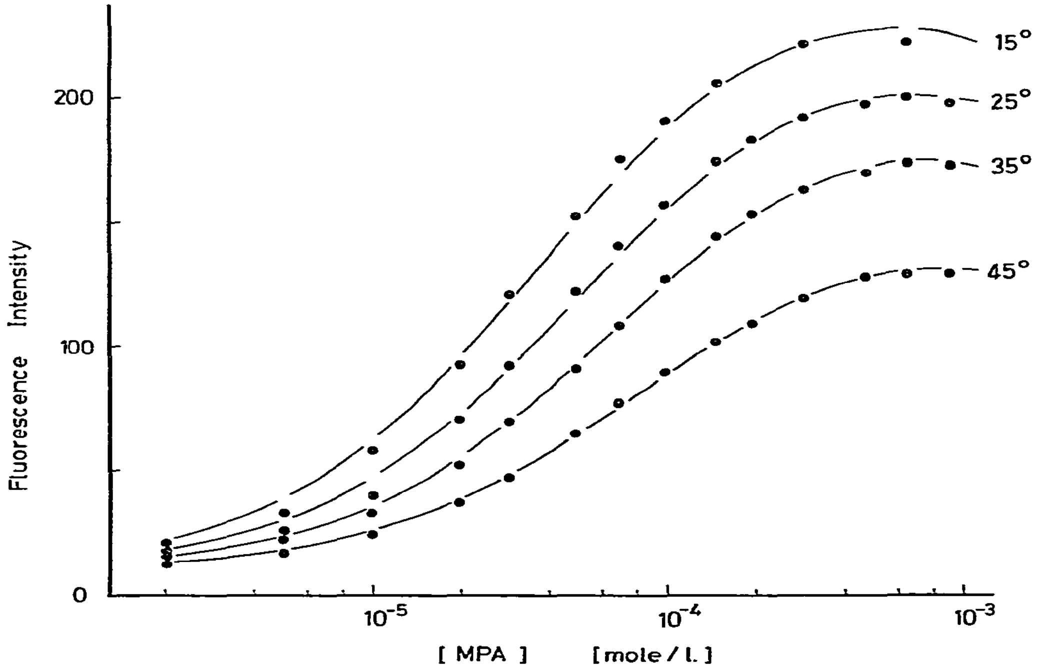

Fig. 2. Representative curves for the titration of NPN with intensely-sonicated C_{12}-MPA. ([NPN], 5×10^{-6} M; [NaCl], 0.1 M; pH 8; details, see sect. 3.2). The curves are theoretical, based upon best-fit values from table 1. The slight decrease at high [MPA] is due to dilution. The fluorescence units are arbitrary and consistent with those in figs. 4, 15 and 16 and in table 1.

Table 1
Binding constants for C_N-MPA and NPN

	N	T°C	[NaCl]	$\log_{10}K$	ΔF_{max}
(i)	12	35.0	0 (f)	4.187	211
	12	35.0	0.01 (g)	4.224	219
	12	35.0	0.100	4.240	244
	12	35.0	0.300	4.257	228
	12	35.0	0.500	4.292	234
	12	35.0	0.700	4.318	235
	12	35.0	1.00	4.336	244
	12	35.0	2.00	4.45 (h)	231
(ii)	12	70.0	0.100	3.653	158
	12	70.0	0.100	3.647	157
	14	70.0	0.100	3.684	168
	14	70.0	0.100	3.717	158
	16	70.0	0.100	3.686	139
	16	70.0	0.100	3.669	150
	18	70.0	0.100	3.710	156
	18	70.0	0.100	3.747	151
(iii)	12	44.6	0.100	4.090	149
	12	35.5	0.100	4.182	199
	12	25.2	0.100	4.305	226
	12	15.3	0.100	4.431	254
(iv)	12	29.9	0.100 (a)	4.291	219
	12	29.9	0.100 (b)	4.140	200
	12	29.9	0.100 (c)	4.012	215
	12	29.9	0.100 (d)	3.912	205
	12	29.9	0.100 (e)	3.817	214

Parameters: K is the observed binding constant (see eq. (1)). ΔF_{max} is the change in fluorescence intensity (uncorrected for absorption, see text) accompanying the change from fully aqueous to fully membrane-bound NPN.
Units: N, the number of carbon atoms in the fatty acid chain of the MPA; [NaCl], M; K, M^{-1}; F, arbitrary units of fluorescence intensity (mm. deflection of the pen recorder at fixed instrument settings; F units are the same in the whole of this paper).
Conditions: [NPN], 5×10^{-6} M; disodium monohydrogen phosphate, 10^{-3} M; (a)–(e), series containing in addition 0%, 30%, 40%, 50% and 60% sucrose respectively (weight/volume); (f) disodium hydrogen phosphate, 5×10^{-4} M, hence effective 1 : 1 salt is 10^{-3} M; (g) ionic strength 0.012 M; (h) strong light-scattering due to the high salt concentration made this result too inaccurate for use.

$$F = F_0 + \Delta F_{max} \cdot \frac{K[\mathrm{MPA}]}{1 + K[\mathrm{MPA}]} \cdot \frac{2}{2+v}$$
$$= F_0 + \Delta F \frac{2}{2+v} \qquad (2)$$

Binding constants obtained under various conditions are set out in table 1. They make manifest (i) the effect of salt concentration on the binding of NPN to C_{12}-MPA, (ii) the effect of chain length upon NPN binding to C_{12}- to C_{18}-MPA, (iii) the effect of temperature upon NPN binding to C_{12}-MPA and (iv) the effect of sucrose upon NPN binding to C_{12}-MPA. The latter two sets of measurements were made in order to evaluate the kinetic data; conclusions from the others will be discussed in sect. 4.1. While series (i) was made at the arbitrary, convenient temperature of 35°C, series (ii) has to be measured at a temperature well above the phase transition temperature of C_{18}-MPA, which is 61°C. Consequently 70°C was chosen for this series.

As before, in all these titrations MPA is in great excess over bound NPN, so that mutual interaction between bound NPN molecules is negligible. In fact, the low solubility of NPN in water implies a restricted solubility in the lipid membrane, since when one of these phases is saturated, the other will be too if the system is in equilibrium. An experiment to see how far the NPN could be forced into the membrane is shown in fig. 3. Here a Job's plot is employed, with the sum of the NPN and MPA concentrations equal to 3×10^{-5} M, which is the highest possible value of this sum, since the NPN concentration in water cannot exceed ca. 3×10^{-5} M and even this is a supersaturated solution (see sect. 2.4). The slight asymmetry of the Job's curve shows that the interaction between MPA and NPN is indeed not a simple solute-solvent relationship; this point is discussed further below (sect. 4.3).

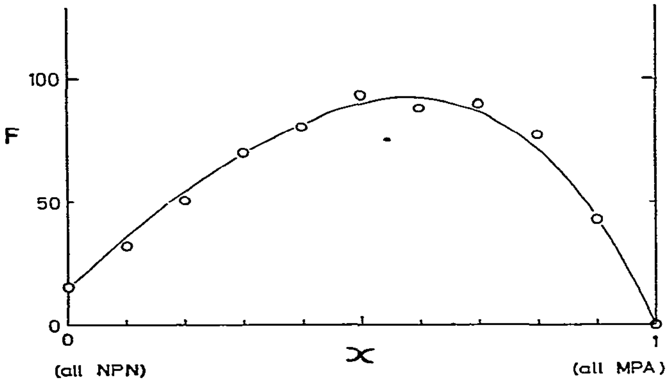

Fig. 3. Job's plot for NPN binding to C_{12}-MPA (see sect. 4.1). [MPA] + [NPN] = 3×10^{-5} M; x = mole fraction of MPA. The curve is theoretical (sect. 4.3).

3.2. Equilibrium binding of NPN to ordered MPA

C_{14}-MPA was used for this study at acidic and alkaline pH. Since a comparison was required between the modes of binding to the crystalline and to the liquid-crystalline forms of the lipid membrane, the dispersions were sonicated in the gentler manner (sect. 2.3); violent sonication is unsuitable for studies below the phase transition temperature (sect. 4.1). Consequently light-scattering interfered to some extent with the measurement of the fluorescence signal and the titration curves were somewhat misshapen, with a resulting uncertainty in the binding constant. Under the conditions of the titrations MPA was always in great excess over bound NPN, so that saturation of the lipid is not approached. Fig. 4 shows the curves and table 2 the constants obtained; the better curves allowed the binding constant to be found from a plot of $\Delta F/[\mathrm{MPA}]$ against ΔF (cf. eq. (2)). The absolute value of the gradient of such a plot is equal to the binding constant and the intercept on the horizontal axis is $\Delta F_{\max}$, i.e., the difference between the fluorescence intensities of membrane-bound and aqueous NPN at the given concentration. Where complete binding of the NPN was not nearly attained, the deviation from the theoretical form was greatest; however, rough values of the binding constants could be read off from the points of inflection of the titration curves.

Table 2
Approximate binding constants for C_{14}-MPA and NPN

pH 8.9			pH 2		
T°C	$\log_{10}K$	Q	T°C	$\log_{10}K$	Q
63.5	3.70	0.47	73.7	3.60	0.13
49.2	3.93	0.51	61.6	3.76	0.19
34.8	4.08	0.54	51.2	3.93	0.25
20.5	3.01	~0.5	20.7	3.12	~0.4
11.0	3.11	0.51	6.8	3.40	~0.4
3.0	3.21	~0.5			

Units: K, M^{-1}; Q, absolute quantum yield based on the standard value of 0.22 in methanol [10].

3.3. Solubility of NPN in NaCl solutions

Table 3 shows the experimental data obtained and the final column gives the solubility of NPN at the salt concentrations used. The "salting-out" of the nonelectrolyte is clear. The difference in free energy of solution caused by changing the salt concentration from 1 mM to 1 M is 490 cal/mole. The surface energy of pure water is 72.75 erg/cm^2 and that of molar

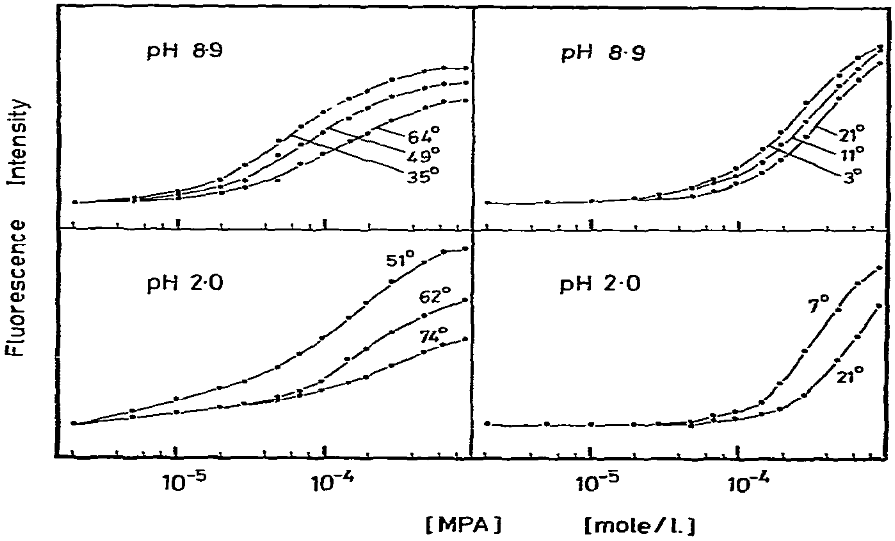

Fug. 4. Curves for the titration of NPN with gently-sonicated C_{14}-MPA. ([NPN], 5×10^{-6} M; [NaCl], 0.1) The curves are empirical.

Table 3
Solubility of NPN in sodium chloride solution

[NaCl]	Absorbance (a)	ϵ_{218}	Absorbance (b)	Solubility
0.001	0.458	4.78×10^4	0.324	6.78×10^{-6}
0.010	0.542	5.65×10^4	0.332	5.88×10^{-6}
0.100	0.573	5.97×10^4	0.270	4.52×10^{-6}
0.300	0.560	5.84×10^4	0.245	4.20×10^{-6}
0.500	0.533	5.56×10^4	0.206	3.71×10^{-6}
0.700	0.496	5.17×10^4	0.159	3.08×10^{-6}
1.000	0.453	4.72×10^4	0.139	2.94×10^{-6}

Units: [NaCl], M; ϵ, cm^{-1} M^{-1}; solubility, M.
(a) at 9.6×10^{-6} M and 30°C. (b) at concentration corresponding to saturation at 20°C; measured at 30°C.

sodium chloride solution is 74.53 erg/cm^2 (data for 20°C, interpolated from ref. [11]). If the surface tension of the NPN–water interface is not too different from that of the air–water interface, then a simple calculation shows that the change in area of this interface when one NPN molecule dissolves in water is around 190 $Å^2$. This is a reasonable value for the surface area of a molecule such as NPN, confirming the reliability of the solubility measurements.

3.4. N.M.R. measurements

Proton magnetic resonance spectra were run by H. Füldner on a Bruker 270 Mc/s Fourier transform spectrometer. The dispersions were prepared according to the intensive sonication procedure described; samples contained 1 ml of 0.1 M MPA in the presence of 0.002 M marker (sodium $d_4$3-(trimethylsilyl)-propionate, Merck UVASOL grade; chemical shift taken as zero) and 0.01 M sodium carbonate to keep the pH high. Spectra were taken at 2°C and 25°C; the former, below the transition temperature, gave better resolution, but were of no value in the binding studies. To observe the effect of NPN on the MPA spectrum, 50 μl of 0.5 M NPN in deuteromethanol was added. Some NPN was precipitated, so the result cannot be evaluated quantitatively. The chemical shifts observed along with their assignments are shown in table 4.

3.5. Light-scattering measurements

These were carried out by Dr. S. Morris using a Fica 50 light-scattering instrument, in order to check that the titration measurements were not being overlaid by the onset of micelle formation in the region of low MPA concentration. Substantial scattering

Table 4
The effect of NPN upon the chemical shifts of MPA protons

Peak	$\delta(1)$	$\delta(2)$	$\delta(2)_{corr.}$	$\Delta\delta$
Marker	0	0	0	–
Fatty-acid ω-CH_3	0.928	0.885	0.881	−0.047
Fatty-acid $C{-}CH_2{-}C$	1.329	1.282	1.276	−0.053
Fatty-acid α-CH_2	2.388	2.257	2.247	−0.141
$P{-}O{-}CH_3$	3.603	3.565	3.549	−0.054
$-CH_2{-}O{-}P$	4.254	4.186	4.167	−0.087
$-O{-}CH_2{-}C$	4.493	4.412	4.392	−0.101
H_2O	4.804	4.826	4.804	–
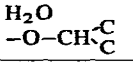 $-O{-}CH{<}^{C}_{C}$	5.324	5.261	5.237	−0.087

Key: chemical shifts in parts per million. $\delta(1)$ was measured without NPN and $\delta(2)$ after the addition of NPN in methanol, $\delta(2)_{corr}$ has been corrected for the change in bulk diamagnetic suspectibility caused by the methanol and NPN. It is obtained by scaling the chemical shifts $\delta(2)$ so as to bring that of water back to 4.804. $\Delta\delta$ is the difference between $\delta(2)_{corr}$ and $\delta(1)$.

amplitudes at lipid concentrations below 10^{-6} M (using as a blank water from the same source as was used to make up the dispersions) demonstrated that the critical micelle concentration of MPA lies well below this value, so that micellation did not interfere with the titrations.

4. Discussion

It has frequently been observed (especially by U. Strehlow, personal communication) that the intensity of the fluorescence signal from NPN bound to fluid (liquid-crystalline) MPA is insensitive to the previous handling of the dispersion (intense or mild sonication, or none at all). On the other hand the intensity of the fluorescence signal from the same system cooled below the phase transition temperature varies markedly; the ratio of intensities above and below the transition can be as low as 2 : 1 following violent sonication and can approach 10 : 1 if sonication has been avoided. This behaviour suggests that a large contribution towards the binding of NPN to ordered MPA is made by the uptake of dye molecules into lattice defects in the ordered MPA structure. In a comparison between binding above and below the transition it was therefore desirable to use a very mild sonication procedure, in spite of the sacrifice of accuracy necessitated thereby.

4.1. Binding to fluid MPA

Here it was possible to minimise light-scattering, and thus to keep accuracy high, by utilising the standard sonication procedure (see sect. 2.3) known to produce small vesicles which show a normal ordered-fluid phase transition at the correct temperature, i.e., which contain bilayers; although these are structurally imperfect in the solid state they should suffice for measurements on the fluid state. Binding constants obtained for NPN to C_{12}-MPA in the presence of 0.1 M sodium chloride (fig. 2 and table 1 (iii)) are displayed in fig. 5 as a van 't Hoff plot, from which an enthalpy of binding of −4.88 kcal/mole and an entropy of binding of +3.36 cal/deg-mole are obtained. The association of highly apolar molecules in water is normally driven by entropy and weakly opposed by enthalpy, whereas the association of moderately apolar molecules is driven by enthalpy and weakly opposed by entropy [12]. Here the association is almost entirely enthalpy-driven, but both enthalpy and entropy have quite small absolute values in comparison with more extreme cases (e.g., micellar association, with ΔH around 5 kcal/mole and ΔS around 30 cal/mole-deg [13] or self-association of dyes, with ΔH around 25 kcal/mole and ΔS around 50 cal/mole-deg [14]). It is therefore reasonable to regard NPN binding to MPA as an intermediate case.

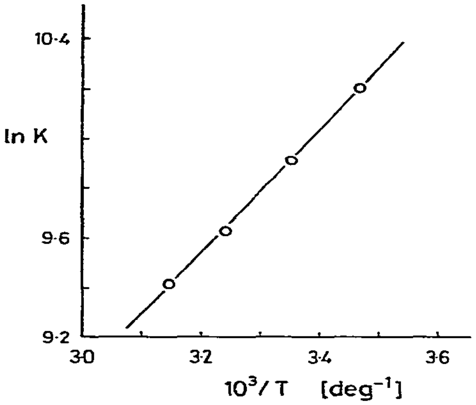

Fig. 5. Van 't Hoff plot for NPN binding to C_{12}-MPA (data from table 1).

The thermodynamics of binding yield no insight into the question of the location of the bound NPN. A priori there are many conceivable positions which the bound dye could adopt: (i) flat across the surface of the membrane, separating the membrane from the water; (ii) between the methyl phosphate head-groups but not reaching further into the membrane than the glyceryl ester groups; in a fixed position between the glyceryl ester groups, extending either (iii) out into the water phase or (iv) into hydrocarbon layer; (v) distributed randomly inside the hydrocarbon layer; (vi) in the cleavage plane between the ends of the hydrocarbon chains of the bilayer, either lying parallel to this plane or in a random orientation. We wish in the following discussion to throw some light on this question.

The effect of added salt on the binding of NPN to MPA will be twofold: (i) it will "salt out" the dye into the membrane; (ii) it will reduce electrostatic repulsion between the lipid head-groups. The latter effect should not affect the binding if the NPN molecule

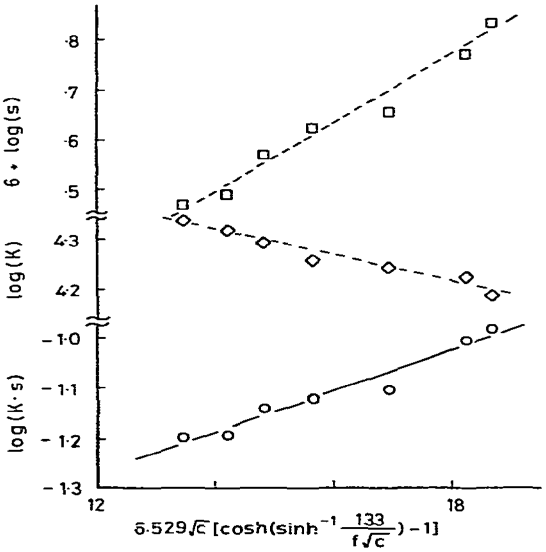

Fig. 6. Effect of sodium chloride on the solubility and the binding to C_{12}-MPA of NPN. For explanation, see sect. 4.1. The solid curve is the best-fit straight line, corresponding in the theoretical model to a molecular area of 40.6 Å^2 for NPN; the hatched lines do not correspond to any theoretical model.

does not contribute to the area of the membrane, but if the NPN binding expands the membrane then the latter effect will reduce the binding constant as salt is added. The magnitude of the latter effect upon the logarithm of the binding constant is given in appendix 1, eq. (A7). Since the standard free energy of transfer of one mole of dye from solution to membrane is $-RT \ln K$, where K is the binding constant, and the standard free energy of transfer[‡] of one mole of dye from crystalline NPN to water is $-RT \ln s$, where s is the solubility, binding constants to MPA can be referred to the solid state by adding the logarithm of the solubility of the dye in water to the logarithm of the binding constant; this corrected binding constant will not suffer from variations due to "salting-out". Eq. (A7) is linear in the area (f_g) occupied by the dye in the membrane, so a plot of the corrected $\log K$ against the function of concentration shown should yield a straight line of gradient f_g. Such a plot is shown in fig. 6, in the construction of which a value of 46 Å^2 for f (the molecular area of MPA) has been assumed (A. Blume and K. Harlos, personal communication). In this figure $\log K$ and $\log s$ are also shown. The gradient of the plot of ($\log K + \log s$) is 41, implying that a single NPN molecule expands the fluid MPA membrane on one side by 41 Å^2 or on both by 20.5 Å^2; since the maximum length of an NPN molecule is 13 Å it cannot extend across the bilayer, so we shall discount the latter possibility.

The effect of chain length upon the binding constant for NPN binding to MPA's of chain length C_{12} to C_{18} is shown in fig. 7. The eight points regress to a straight line having a gradient of 120 ± 40. The interpretation of this is as follows: a point solute in the interior of a bilayer composed of lipids with chain length N, with freedom to move randomly in the region of the carbon chains but not outside it, would show a binding constant K_N proportional to N; thus K_{18}/K_{12} would equal 1.5. If, for example by virtue of the apolarity of the molecule, its centre were excluded from the region of the outermost N' chain carbon atoms, then K_{18}/K_{12} would equal $(18-N')/(12-N')$, i.e., would exceed 1.5. Conversely, if the guest molecule were confined to a region of fixed volume, irrespective of chain length, then K_{18}/K_{12} would equal one. In fact, as fig. 7 shows, the value of this ratio is 5250/4540 = 1.16. The expected gradient for a K_{18}/K_{12} value of 1.5 would be 330, shown as a hatched line in fig. 7. Thus although the gradient is not zero, it does not nearly approach the minimum value compatible with the free movement of NPN in the hydrocarbon interior of the MPA membrane. The

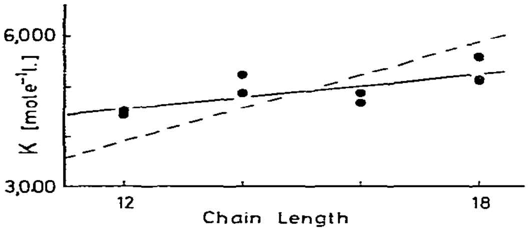

Fig. 7. Chain-length dependence of the binding constant for NPN/MPA (data from table 1 (iii)). The abscissa corresponds to N in fig. 1. Full line: best-fit straight line; hatched line: theoretical gradient for uniform distribution of the NPN throughout the membrane (see sect. 4.1).

[‡] Strictly, an arbitrary constant should be added here, since standard states in the membrane have not been defined.

deviation of the gradient from zero points to a partition between these types of "confined" and "free" NPN molecule in the membrane, with the former predominating.

Of the six possible modes of binding listed above, we can now eliminate all but one. An increase in the area of the membrane is not compatible with positions (i) and (ii), and the observed magnitude of this expansion, 41 Å^2, is about equal to the area which an NPN molecule in the membrane surface might take up, so this figure supports positions (iii) and (iv) most strongly. A consideration of the non-polar nature of NPN and of the thermodynamic parameters of the binding also makes (i) and (ii) unlikely, and this conclusion is reinforced by the high fluorescence quantum yield and short fluorescence emission wavelength of the bound dye (ref. [1]). The near-independence of chain length shown by the binding constant rules out position (v). Inspection of the changes in chemical shift induced by the NPN ring currents in the MPA protons (table 4) shows that the effect is greatest upon the α-CH_2 groups of the fatty acid chains and least upon the ω-CH_3 groups. Thus position (vi) is not the principal site of NPN binding. The binding is thus best described by position (iii) or (iv); since formation of a hydrogen bond in a nonpolar medium can release substantial amounts of free energy [15] it is probable that the N—H group is bound to the phosphate group of an adjacent lipid molecule, causing the NPN molecule to lie with its "plane" (NPN is not exactly planar, owing to steric interference between the two rings) parallel to the lipid chains and the phenyl ring possibly forced by the geometry of the molecule some way towards the $^-O_3POCH_3$ groups. This is consistent with the observation that while the indicator ANS, which is identical to NPN except in that it bears a negatively-charged sulphonate group, binds to lecithin by residing between the zwitterionic choline phosphate groups [16,17], showing a strong N.M.R. interaction with the choline methyl protons, the region of NPN binding to lecithin is remote from these protons [18].

In view of the small but finite chemical shift of the ω-CH_3 protons caused by NPN (table 4) and the positive slope seen in fig. 7, it seems likely that while most of the bound NPN molecules reside between the glyceryl ester groups, a small number pass into the very interior of the membrane, confirming the conclusion drawn above from the binding studies.

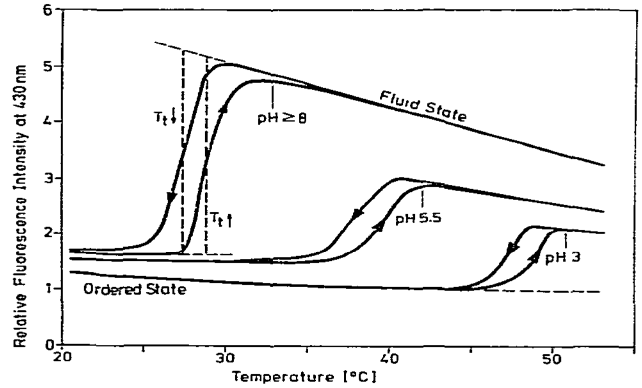

Fig. 8. Thermal transition curves for MPA at different pH values, monitored by NPN fluorescence ([NPN], 10^{-6} M; [MPA], 10^{-4} M; [NaCl], 5×10^{-3} M; [EDTA], 10^{-4} M). The three curves were measured with the same dispersion and with identical instrument settings. Taken from ref. [4].

4.2. Binding to ordered MPA

In spite of frequent use of NPN as an indicator of the crystalline—liquid—crystalline transition in MPA, the cause of the increase in fluorescence at the transition has not been investigated, and the reason for the considerably greater fluorescence signal obtained from NPN in the presence of fully-ionised MPA in comparison with that obtained when the MPA is protonated is likewise not known. Both effects are shown in fig. 8, from ref. [4]. The binding constants of NPN to C_{14}-MPA above and below the phase transition were therefore determined at bulk pH values 8.9 and 2.0. The results are expressed as a van 't Hoff plot (fig. 9) and lead to the following inferences:

(i) The binding constants measured at alkaline pH in the absence of salt are greater than those measured at the same pH in 0.1 M sodium chloride, in accordance with the results obtained with C_{12}-MPA.

(ii) The binding constants measured with 0.1 M salt were unaffected by the change in pH from 8.9 to 2.0. This is not in accord with the electrostatic theory, since the MPA should be largely neutralised at the latter pH value [4], so the binding constant at pH 2.0 should be appreciably lower than at pH 8.9 (according to eq. (A7), by a factor of at least 2.5 if f_g is 41 Å^2 and the lipid is at least half protonated). This

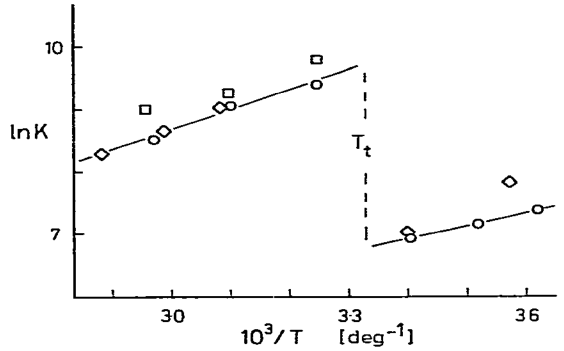

Fig. 9. Van 't Hoff plot for NPN binding to C_{14}-MPA (data from table 2 and preliminary experiments). Circles: pH 8.8, [NaCl] 0.1 M; squares, pH 8, NaCl not added; diamonds, pH 2.0, [NaCl] 0.1 M. The two straight lines are drawn through the two sets of circles. T_t is the transition temperature for C_{14}-MPA at pH 8.8; the value for pH 2.0 (not shown) lies 1.5 scale divisions to the left of this.

discrepancy is surprising, but it is not due to experimental error. It may reflect the onset of protonation of the very weakly basic nitrogen atom of NPN; this would strengthen the binding to the residual negative charge on the MPA.

(iii) At the phase transition the binding constant changes by a factor of ca. 20. In contrast with this the quantum yield of the bound NPN does not change significantly at the phase transition (table 2). The indication of the transition by NPN is therefore due entirely to the release of bound NPN into solution when the fluid membrane becomes ordered, and not to a change of binding site. Although the determinations at pH 2.0 were less accurate than those at pH 8.9, owing to interference by light-scattering, the same decrease in binding constant is seen for protonated as for fully deprotonated MPA.

(iv) In consequence of this the observed decrease in fluorescence intensity when fluid MPA is protonated cannot be due to the expulsion of bound NPN and must be due to a change in quantum yield of the NPN, which remains bound. This is confirmed by inspection of table 2, which shows a decrease in quantum yield of bound NPN upon protonation of the host MPA by a factor of about 2.5, and with the observation (fig. 8, taken from ref. [4]) that the effect of protonation is greater upon NPN bound to fluid than to ordered MPA. This effect provides further confirmation for the conclusion (sect. 4.1) that most of the NPN is bound into the surface of the MPA membrane, since a guest molecule in the non-polar interior of the membrane could not experience the field gradient at the surface. Another possible factor is protonation of the NPN.

The sensitivity (see beginning of sect. 4) of the fluorescence signal from NPN in ordered, but not in fluid, MPA to the previous mechanical treatment of the dispersion suggests that the signal from NPN in ordered MPA does not in fact originate from "ordered" MPA at all, but instead comes from NPN molecules bound to lattice defects or domain boundaries in the MPA crystal structure. In the presence of excess MPA the concentration of such disordered regions would be proportional to the concentration of lipid, and under the conditions of the experiments described here the binding of dye to such regions below the transition would manifest itself as a reduced binding constant, the amount of the reduction depending upon the amount of disorder, i.e., upon the previous treatment of the sample. This description of the binding of NPN to MPA below the phase transition temperature is consistent with all the data and, if correct, implies that interpretation of binding data below the transition should in general be made with caution, since such data could well refer to dye binding to small, fluid regions unrepresentative of the ordered lipid as a whole.

4.3. Stoichiometry of NPN binding to fluid C_{12}-MPA

Until now all discussion has centred upon the binding of NPN to an excess of MPA. Since the concentration of MPA has always been far greater than that of bound NPN, it has been possible to use an empirical binding constant defined in eq. (1). If the approximation $[\mathrm{MPA}] \gg [\mathrm{NPN_{bound}}]$ breaks down then saturation of the lipid commences, and eq. (1) has to be replaced with eq. (3), where m is the number of lipid molecules making up the binding site of one NPN molecule and K_{tr} the "true" binding constant, i.e., that measured if the lipid concentration is expressed in moles per litre of groups of m lipid molecules (m need not be an integer). [MPA] refers in eq. (3) as in eq. (1) to the total concentration of lipid molecules. Since eq. (1) is a special case of eq. (3), we can show by considering an excess of MPA that K is equal to K_{tr}/m.

$$K_{tr} = \frac{[\mathrm{NPN_{bound}}]}{[\mathrm{NPN_{free}}]} \cdot \frac{1}{([\mathrm{MPA}]/m - [\mathrm{NPN_{bound}}])} \qquad (3)$$

In the Job's plot the sum of NPN and MPA concentrations is held at a constant value Σ; these are expressed by a parameter x according to eqs. (4). If the concentration of bound NPN is denoted by y then y is given by the quadratic equation (5), obtained by substitution of eqs. (4) into eq. (3).

$$[\mathrm{MPA}]_{\mathrm{total}} = x\Sigma; \qquad [\mathrm{NPN}]_{\mathrm{total}} = (1-x)\Sigma \qquad (4)$$

$$y^2 mK - y(1 + xK\Sigma + mK(1-x)\Sigma) + Kx(1-x)\Sigma^2 = 0 \qquad (5)$$

The corrected fluorescence intensity is proportional to the concentration of the fluorescing species. If the molar fluorescence intensities of free aqueous NPN and MPA-bound NPN are $\bar{F}_a$ and $\bar{F}_b$ respectively, and F_c is the observed corrected signal, then use of eqs. (4) leads to eq. (6), so that the function $f(F_c)$, defined in eq. (7), is linear in y.

$$F_c = \bar{F}_a((1-x)\Sigma - y) + \bar{F}_b y \qquad (6)$$

$$f(F_c) = F_c - (1-x)\bar{F}_a\Sigma = y(\bar{F}_b - \bar{F}_a) \qquad (7)$$

This function contains no adjustable parameters other than m, since K and $(\bar{F}_b - \bar{F}_a)$ are known from the titrations with excess MPA ($(\bar{F}_b - \bar{F}_a) = \Delta F_{\mathrm{max}}/[\mathrm{NPN}]_{\mathrm{total}}$) and $\bar{F}_a$ can be determined independently using NPN solutions without lipid. Therefore by assuming a value for m one can find y from eq. (5) as a function of x; the linearity of a plot of $f(F_c)$ against y and the closeness of the gradient $(\bar{F}_b - \bar{F}_a)$ to the value obtained from titration provide a measure of the correctness of the value assumed for m. Such plots are shown in fig. 10 for m values of 1, 4.5 and 10. The best fit (least-squares regression onto a line passing through the origin) was obtained with m equal to 4.5; this value gave a fit slightly better (standard deviation of the gradient 1.01) than did m values of 4 or 5 (S.D. 1.1) and decidedly better than did m values of 3 or 6 (S.D. 1.6 and 1.4). The gradient obtained for m = 4.5 is 47.2 fluorescence units per μM, in good agreement with the value from the titrations, namely 47.6 fluorescence units per μM after correction for UV-absorption and interpolation to 30°C (cf. table 1, in which the change in fluorescence intensity is expressed in the same units for 5 μM NPN).

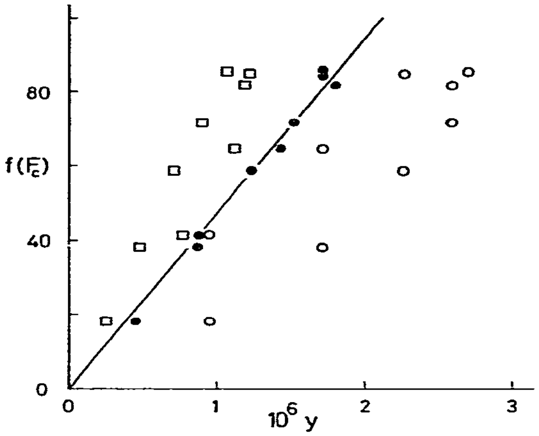

Fig. 10. Linearised form of the Job's plot in fig. 3, based on eqs. (7) and (5). See sect. 4.3. Squares, m = 10; full circles, m = 4.5; open circles, m = 1.

In addition to the Job's plot a titration was carried out in which NPN was added to a low concentration of MPA in order to drive as much dye as possible into the lipid. The accurate addition of very small amounts of NPN in methanol to the titration cell is experimentally very difficult, so this titration cannot be interpreted with exactitude. The result is shown in fig. 11 as a plot of corrected fluorescence intensity against the concentration of NPN added. The theoretical curves, derived as indicated above, correspond to various values of m; all other parameters were as in the last experiment. Best fit is obtained for m = 3, in rough agreement with the value from the Job's plot. We consider the latter to be more reliable, since there is less room for systematic error. However, there is a further reason for uncertainty, which lies in the fact that the groups of m MPA molecules involved in binding one NPN molecule are not independent of one another. Thus an incoming NPN molecule "sees" a far greater number of permutations of lipid molecules in the membrane surface, each permutation making up a potential binding site, when the membrane is almost unoccupied by other NPN molecules than when it is almost saturated. This leads to a complex situation of mutual exclusion, possibly influenced further by co-operativity, for which a quantitative description so far exists only for binding to a one-dimensional

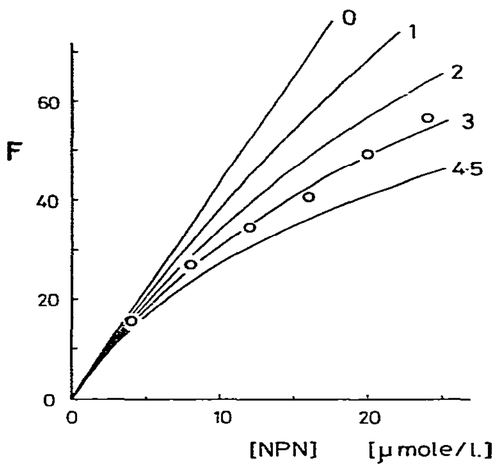

Fig. 11. Titration of MPA with NPN. The curves are theoretical, based on known binding strength and fluorescence intensity, and assuming m-values of 0, 1, 2, 3 and 4.5 (see sect. 4.3). ([MPA], 5×10^{-6} M; [NaCl], 0.1 M; 30°C).

polymer [19]; qualitatively, it is clear that increasing the saturation of the membrane with NPN reduces the apparent binding constant or appears to increase m. In addition, complications will arise if two NPN molecules can lie next to one another in the MPA membrane; this will reduce the average value of m at high degrees of saturation. However, the restricted ability of MPA to incorporate NPN (sect. 3.1) shows that such complications are not of great importance.

In conclusion of the discussion of the stoichiometry of NPN binding to MPA, two further points should be made in order to remove any ambiguity in the interpretation of the Job's plot. Firstly, at high dilution eq. (5) may be simplified, since the y^2 term vanishes ($y^2 \ll \Sigma^2$), as do the two terms in the bracket containing Σ ($\Sigma \ll 1$). Rearrangement yields eq. (8), which does not contain m, so that m is indeterminate and the function $f(F_c)$ shows a maximum at $x = 1/2$ irrespective of the nature or the stoichiometry of binding. This can lead to the false inference of a 1 : 1 stoichiometry. Only in cases where saturation is achieved can the stoichiometry of the binding reaction be read off from the maximum in the Job's plot, and only where saturation is approached can m be determined at all.

$$y = x(1 - x)K\Sigma^2 \tag{8}$$

Secondly, a further possible model for the dye binding which we have not yet discussed is the partition of the dye between one liquid (water) and another (the interior of the membrane). If this partition is described by a partition coefficient c, the volume of the aqueous phase is V, the volume of the interior (oil) phase is v and the volume of the oil phase per mole of MPA is v_0, then combining relationships (4) with the partition law gives eq. (9).

$$c = \frac{[\mathrm{NPN_{oil}}]}{[\mathrm{NPN_{free}}]} = \frac{yV/v}{(1 - x)\Sigma - y} \tag{9}$$

$$-y(1 + v_0 cx\Sigma) + v_0 cx(1 - x)\Sigma^2 = 0 \tag{10}$$

Introducing the relationship $v = Vv_0x\Sigma$ leads to eq. (10), which is analogous to eq. (5), insofar as comparison of eq. (9) with eq. (1) under conditions where eq. (1) holds (excess MPA) shows that v_0c equals K. Eq. (10) might thus equally well have been obtained by placing $m = 0$ in eq. (5), implying that in liquid/liquid partition no liquid molecule is "consumed" by the entry of solute, in consequence of which the ratio of concentrations of solute in the two phases remains independent of their sum (cf. fig. 11, for the case where $m = 0$). Now at low Σ values eq. (10) reduces, just as eq. (5) does, to eq. (8), so that again no information about the binding is obtainable at low Σ values.

Furthermore it may be shown by differentiation of eq. (10) or by insertion of values that at higher concentrations $f(F_c)$ for the partition model passes through a maximum only in the region $0 < x < 1/2$, whereas inspection of fig. 3 shows that this is not the case (in fig. 3 F_c is plotted rather than $f(F_c)$, but the difference is small and the maximum not noticeably shifted). The liquid/liquid partition model of NPN binding can therefore be eliminated.

4.4. Equilibrium binding: conclusions

The NPN is bound into the surface of the MPA; its environment is predominantly non-polar and it resides in the region of the carboxylate ester groups. There is little if any partitioning of NPN molecules into the very interior of the bilayer. The binding enthalpy of one mole of NPN to excess fluid C_{12}-MPA is −4.9 kcal and the entropy +3.4 cal/deg; the binding of one molecule expands the membrane by 41 $Å^2$, the effective area of the NPN molecule in the bilayer. Consistently with this effective area, the effective "binding site" for an NPN molecule comprises approximately four MPA molecules. When the lipid adopts the ordered state the binding constant for NPN decreases greatly, and this is the origin of the usefulness of NPN as an indicator of the phase transition; the fluorescence quantum yield of the indicator is unaffected by the transition, but is affected by the surface charge on the MPA. It is possible that NPN bound to MPA below the transition temperature resides exclusively in regions of local disorder rather than in the crystalline areas. Electrostatic theory predicts correctly the dependence of the binding constant of NPN to fluid, fully-ionised MPA upon the external salt concentration, but not upon the external pH, where further factors (e.g. protonation of the dye) may play an important and as yet unexplored rôle.

Acknowledgements

Particular thanks are due to Dr. H. Eibl for guidance in the synthesis of the lipids. I also thank Dr. U. Strehlow for providing details of sonication, Dr. S. Morris and H. Füldner for making specialised measurements, Mrs. U. Sievers for conducting the C_{14}-MPA titrations, Dr. H. Diebler for discussion and Professor M. Eigen for encouragement and support.

Financial support from (in chronological order) the Alexander von Humboldt Foundation, the Max-Planck Society, E.M.B.O. and Magdalene College is gratefully acknowledged.

Appendix I

The effect of membrane electrostatics on the binding of a neutral molecule

We consider a lipid whose molecules in the bilayer occupy an area f. A neutral guest molecule is bound whose area is f_g. This results in an expansion of the membrane, so that the surface charge density and surface potential of the membrane are lowered. The resulting change in the electrostatic contribution to the free energy of the system is therefore reflected in the binding constant of the guest molecule.

Let the degree of dissociation of the head groups on the membrane be α, resulting in a surface density of charge σ and a surface potential ψ_0. Let the concentration of ambient 1 : 1 electrolyte be C. If k is the Boltzmann constant, e the electronic charge, L Avogadro's number, T the absolute temperature and ϵ_0 and ϵ_r the permittivity of free space and the dielectric constant of water, respectively, then from the Gouy-Chapman equations [4,20] in S.I. units σ and ψ_0 are related by eq. (A1).

$$\frac{e\alpha}{f} = \sigma = (8\,C\epsilon_r\epsilon_0 kT)^{1/2} \sinh \frac{e\psi_0}{2kT} \qquad \text{(A1)}$$

The free energy of the membrane is given [4] by

$$G = G^* + G^{\mathrm{el}} \qquad \text{(A2)}$$

eq. (A2), which embodies the assumption that the electrostatic charge on the membrane results in a free energy term G^{el} which may be added to the free energy which the same membrane would have if it were uncharged. This is discussed in detail in refs. [4] and [21]. G^{el} is given by eq. (A3); substitution (eq. (A1)) and integration yield eq. (A4).

$$G^{\mathrm{el}} = Lf \int_0^{\sigma} \psi_0 \, \mathrm{d}\sigma' \qquad \text{(A3)}$$

$$= Lf \left\{ \sigma\psi_0 - \left(\frac{32\epsilon_r\epsilon_0 C k^3 T^3}{e^2} \right)^{1/2} \left(\cosh \frac{e\psi_0}{2kT} - 1 \right) \right\} \qquad \text{(A4)}$$

We now suppose that a small number ($\mathrm{d}N$ moles) of guest molecules becomes bound to one mole of the negatively-charged lipid. The change in free energy of the system is equal to the change that would be experienced if the membrane were neutral, plus a contribution due to the change in electrostatic free energy of the membrane, $\mathrm{d}G^{\mathrm{el}}$. The change in area per charged molecule is given by eq. (A5), from which follows eq. (A6).

$$\mathrm{d}f = f_g \, \mathrm{d}N \qquad \text{(A5)}$$

$$\mathrm{d}G^{\mathrm{el}}/\mathrm{d}N = f_g \, \mathrm{d}G^{\mathrm{el}}/\mathrm{d}f$$

$$
\begin{aligned}
&= f_\mathrm{g} L \int_0^\sigma \psi_0 \, \mathrm{d}\sigma - f_\mathrm{g} L \sigma \psi_0 \\
&= -L f_\mathrm{g} \left(\frac{32 \epsilon_\mathrm{r} \epsilon_0 C k^3 T^3}{e^2} \right)^{1/2} \\
&\times \left(\left[\cosh \left(\sinh^{-1} \frac{e\alpha}{8 f C \epsilon_0 \epsilon_\mathrm{r} k T} \right) \right] - 1 \right) \\
&= -38.49 \sqrt{C} \left(\left[\cosh \left(\sinh^{-1} \frac{133.0\,\alpha}{f\sqrt{C}} \right) \right] - 1 \right) f_\mathrm{g}
\end{aligned}
\tag{A6}
$$

In eq. (A6) conventional values have been inserted for the fundamental constants, with $T = 308$ K, the temperature used in the relevant experiment in this paper; α is unity for a fully-dissociated lipid, as used here, and f and C are expressed in $\mathrm{\AA}^2$ and mole/l respectively. The resulting value in J/mole is the molar electrostatic free energy of binding of NPN to a large excess of MPA.

This treatment is basically the same as that in ref. [4] for an analogous expansion of the charged surface, viz., that at the phase transition from the crystalline to the liquid-crystalline state. Here relatively high salt concentrations are used, so we cannot make use of the approximation previously used for high values of the surface potential.

The binding of NPN to MPA will therefore be reinforced by a free energy term given in eq. (A6). One can express this equally well using the standard relationship $\Delta G = -RT \ln K$ for $\alpha = 1$ in eq. (A7),

$$
\begin{aligned}
\log K &= \log K^* + 6.529 \times 10^{-3} \sqrt{C} \\
&\times \left(\left[\cosh \left(\sinh^{-1} \frac{133.0}{f\sqrt{C}} \right) \right] - 1 \right) f_\mathrm{g}
\end{aligned}
\tag{A7}
$$

where once again C is in mole/l, f and f_g are in $\mathrm{\AA}^2$ and K^* is the binding constant observed under the same conditions with a neutral, otherwise identical membrane. As is seen (see sect. 4.1), K^* can itself be a function of salt concentration, making the observed relationship more complicated than expressed by eq. (A7) alone.

References

[1] H. Träuble and P. Overath, Biochim. Biophys. Acta 307 (1973) 491.

[2] U. Strehlow, Dissertation, Göttingen 1979.

[3] H. Träuble and H. Eibl, in: Functional linkage in biomolecular systems, eds. F.O. Schmitt, D.M. Schneider and D.M. Crothers (Raven Press, New York, 1975) pp. 59–90.

[4] H. Träuble, M. Teubner, P. Woolley and H. Eibl, Biophysical Chem. 4 (1976) 319.

[5] P. Woolley and M. Teubner, Biophys. Chem. 10 (1979) 335.

[6] H. Träuble, in: Structure of Biological Membranes, eds. S. Abrahamsson and I. Pascher (Plenum, New York, 1976) pp. 509–550.

[7] P. Woolley and H. Eibl, F.E.B.S. Lett. 74 (1977) 14.

[8] S. Kovatchev and H. Eibl, in: Enzymes of lipid metabolism, eds. S. Gatt, L. Freysz and P. Mandel (Plenum, 1978).

[9] H. Eibl and P. Woolley, Biophys. Chem. 19 (1979) 261.

[10] G.K. Radda, Biochem. J. 122 (1971) 385.

[11] C.R.C. Handbook of Chemistry and Physics, ed. R.C. Weast (57th Ed., C.R.C. Press, 1976) p. F-43.

[12] W.P. Jencks, Catalysis in chemistry and enzymology (McGraw-Hill, 1969) pp. 418–427.

[13] (a) J.M. Corkill, J.F. Goodman and J.R. Tate, Trans. Farad. Soc. 60 (1964) 996;
(b) M.J. Schick, J. Phys. Chem. 67 (1963) 1796.

[14] Y. Tanizaki, T. Hoshi and N. Ando, Bull. Chem. Soc. Japan 38 (1965) 264.

[15] W.P. Jencks, op. cit., pp. 323ff.

[16] D.H. Haynes and H. Staerk, J. Membrane Biol. 17 (1974) 313.

[17] D.H. Haynes, J. Membrane Biol. 17 (1974) 341.

[18] C.M. Colley and J.C. Metcalfe, F.E.B.S. Lett. 24 (1972) 241.

[19] J.D. McGhee and P.H. von Hippel, J. Mol. Biol. 86 (1974) 469.

[20] R. Aveyard and D.A. Haydon, An introduction to the principles of surface chemistry (Cambridge Univ. Press, 1973) pp. 40–47.

[21] F. Jähnig, Biophysical Chem. 4 (1976) 309.